JOURNAL OF Materials CHEMISTRY

The electronic and magnetic properties of $LaCrO_4$ and $Nd_{1-x}Ca_xCrO_4$ ($x=0$–0.2) and the conduction mechanism

Yoshitaka Aoki,* Hidetaka Konno and Hiroto Tachikawa

Division of Materials Science and Engineering, Graduate School of Engineering, Hokkaido University, Sapporo 060-8628, Japan. E-mail: yaoki@eng.hokudai.ac.jp

Received 3rd October 2000, Accepted 2nd January 2001
First published as an Advance Article on the web 1st March 2001

The electric conductivity of monazite-type $LaCrO_4$ and zircon-type $Nd_{1-x}Ca_xCrO_4$ ($x=0$–0.2) were characterized by measurements of dc electric conductivity and the Seebeck coefficient in the 300–600 K range. The $LaCrO_4$ and $NdCrO_4$ were found to be n-type semiconductors, while commonly known monazite- or zircon-type oxides are insulators. In mixed valence compounds of Cr^V and Cr^{VI}, $Nd_{1-x}Ca_xCrO_4$ ($x=0.1$, 0.2), hole hopping conduction arising from the mixed valency was also observed. The $Nd_{1-x}Ca_xCrO_4$ ($x=0.1$, 0.2) compounds obeyed Curie–Weiss behavior above the Nèel temperature, and the observed magnetic moments for the Cr^V ions were in good agreement with the theoretical values. Experimental results and the calculated spin densities by the UHF method indicated that most of the unpaired electrons from Cr^V were localized on Cr atoms. The *ab initio* MO calculations for CrO_4^{3-} clusters in $NdCrO_4$ revealed that the SOMO is the degenerate $d\pi^*$ state and that the LUMO is the $p\sigma^*$ state (O 2p origin): the SOMO forms the degenerate states at the top of the valence band and the LUMO forms a wide conduction band. For $NdCrO_4$ and $LaCrO_4$ the electronic conduction mechanism as semiconductors was explained by the band model. For $Nd_{1-x}Ca_xCrO_4$ ($x=0.1$, 0.2) electronic conduction was described by the band model combined with hopping conduction of holes in degenerate $d\pi^*$ states. It is concluded that the electronic conductivity of these compounds is caused by an intermixing of the ligand-to-metal charge-transfer (LMCT) state into the ionic configuration.

Introduction

Oxides containing unusual high valence metal ions, such as Cu^{III}, Ni^{III}, Fe^{IV}, Co^{IV} and others, have been studied because of their singular electric or magnetic properties.[1–7] One of the reasons for these interesting properties is the mixing of the ligand-to-metal charge-transfer (LMCT) states, such as $d^{n+1}L$ (L = ligand hole), into the ionic d^n configuration in the ground state.[8] This mixing arises as the energy of the metal 3d states is close to or slightly lower than that of the oxygen 2p states, and as a result the ligand-to-metal charge-transfer energy, Δ, is very small.[8] With increasing formal valence or atomic number in the first transition series, Δ systematically decreases and occasionally becomes negative (negative Δ-type compounds). The unusual high valence state oxides like $NaCuO_2$ and $LaNiO_3$ belong to this category.[5,8]

Rare earth chromates, $LnCrO_4$ (Ln = rare earth), contain unusual high valence state Cr^V ions of the d^1 configuration. Of these, $LaCrO_4$ has a monazite-type structure (monoclinic, $P2_1/n$) but for Ln = Nd–Lu, the $LnCrO_4$ compounds have a zircon-type structure (tetragonal, $I4_1/amd$).[9–12] A number of magnetic studies of $LnCrO_4$ other than of $LaCrO_4$ have been carried out from the point that the Cr^V and Ln^{III} magnetic ions could interact with each other,[13–16] but the electric conductivity of $LnCrO_4$ compounds has not been studied in detail. Recently, it has been reported that Li_3CrO_4 is a semiconductor, despite the zinc blende-related structure which does not have a chain structure between the metal and oxygen atoms and so would generally be assumed to be an insulator.[17] It may be speculated that the high valence state of chromium contributes to the electronic properties of Li_3CrO_4, but no detailed mechanism of conduction has been established.

The authors have reported that both $LnCrO_4$ (Ln = La, Nd) and Cr^V–Cr^{VI} mixed valence compounds, $Nd_{1-x}Ca_xCrO_4$ ($x=0.02$–0.20), can be synthesized as a single phase by pyrolysis of a precursor prepared from mixed solutions of Ln^{III}, Ca^{II} and Cr^{VI}.[9,18] The structure including the atomic positions and the valence state of chromium in these compounds was characterized by X-ray Rietveld refinement, Raman spectroscopy, X-ray photoelectron spectroscopy, and other methods.[9,18] The present work measured the electric conductivity of $LaCrO_4$ and $Nd_{1-x}Ca_xCrO_4$ ($x=0$–0.2), the Seebeck coefficient, and the magnetic susceptibility, and the mechanism of electronic conduction is discussed with *ab initio* MO calculations and structural analysis.

Experimental

Preparation methods, structure, and atomic positions in $LaCrO_4$ and $Nd_{1-x}Ca_xCrO_4$ ($x=0$–0.2) are described elsewhere.[9,10,18] The purity of the samples was determined by titration and XRD measurements.

The electric conductivity was measured in a dry oxygen atmosphere by the dc two-probe method using a disk-shaped sample, *ca.* 12 mm diameter and 4 mm thick, prepared by the CIP method at 100 MPa and sintered at 803 K in O_2 for 72 h. The density of the disks was about 70% of the theoretical density for all compounds because they cannot be sintered at temperatures above 900 K where they decompose: single crystals were not available. There were no differences in the properties of the samples prepared in different runs. Next, both sides of the disks were coated with gold by physical vapor deposition and fine gold wires were connected to the disks with gold paste. The sample was set in an alumina boat and placed on a Pt/Pt-13Rh thermocouple in an electric furnace for the conductivity measurements. Ten data sets with different applied currents at each temperature during heating and cooling cycles were recorded.

The measurements of the Seebeck voltage were carried out with a rod-shaped sample, *ca.* 2 mm diameter and 20–30 mm long, prepared by the method described above. Gold foil was

 DOI: 10.1039/b007968p

attached to both sides of the disks and Pt/Pt-13Rh thermocouples were put around the both ends. The sample was placed vertically in the lower part of a vertical furnace where the temperature gradient was less than 10 K cm^{-1}. To achieve constant contact temperatures, the samples were maintained at the measurement temperature for more than one hour before the measurements of the Seebeck voltage were taken.

The temperature dependence of the magnetic susceptibility was measured at 1000 G by a Quantum Design SQUID magnetometer. Samples were placed in a poly(chlorotrifluoroethylene) container and the signal from the empty container was subtracted from the experimental data.

Ab initio molecular orbital calculations were carried out to calculate the energy diagram of a CrO_4^{3-} cluster by the unrestricted Hartree–Fock method[19,20] on the basis sets of the 6-311+G* level for both atoms in CrO_4^{3-}.[20] The calculations for the dimer and trimer of the CrO_4^{3-} unit were performed on the basis sets of the STO/3G* level for both atoms. The spin density on each atom was calculated by the MP2 method on the basis set of 6-311+G* for both atoms. All calculations were performed using the GAUSSIAN98 program.[19] The calculations used the experimentally determined atomic coordinate data.[9,18]

Results and discussion

Electric properties

A synthesized sample was a single phase, and the average composition and standard deviations are shown in Table 1. All compounds are a type of mono-oxochromate salt: the $Cr^{V}O_4^{3-}$ tetrahedra in $LaCrO_4$ have C_1 symmetry of four different Cr–O bond lengths; the tetrahedra in $NdCrO_4$ have D_{2d} symmetry with four Cr–O bonds of the same length.[9] Structural models are shown in Fig. 1. The mixed valence $Nd_{1-x}Ca_xCrO_4$ ($x=0.02$–0.2) compounds have a structure similar to $NdCrO_4$ and with different lattice parameters.[18] These mixed valence compounds form two types of tetrahedra, $Cr^{V}O_4^{3-}$ and $Cr^{VI}O_4^{2-}$, which are distributed randomly in the zircon-type structure.[18]

The electric conductivity, σ, of $LaCrO_4$ and $Nd_{1-x}Ca_xCrO_4$ ($x=0$–0.2) showed that these oxides have semiconductor characteristics in the 300–600 K range, as shown in Fig. 2(a). The current–voltage relationships were ohmic throughout and no boundary effects were observed in any measurements. The values in Fig. 2(a) are apparent values due to the low density of the samples, but they allow an evaluation of the electric conductivity of the compounds. Plots of the electric conductivity of $LaCrO_4$ and $NdCrO_4$ against the reciprocal of the temperature conform to an Arrhenius-type equation, and the conductivity is in the order of 10^{-5}–10^{-6} S cm^{-1} at ambient temperature, as listed in Table 2, and this is similar to the conductivity of Si.[21] The activation energies obtained from Fig. 2(a) are about 18 kJ mol^{-1} for $LaCrO_4$ and about 20 kJ mol^{-1} for $NdCrO_4$. The electric conductivity of $Nd_{1-x}Ca_xCrO_4$ ($x=0.1$, 0.2) is at least 20 times larger and the activation energy is smaller than with $NdCrO_4$. Fig. 2(b) shows time-variations of σ at 473 K under flowing dry O_2 for $LaCrO_4$ and $Nd_{1-x}Ca_xCrO_4$ ($x=0$–0.2). The variations in σ are very small, indicating that the electric conductivity cannot be attributed to protons or other ionic species and that the carriers in these compounds are electrons or holes.

Table 1 Chemical composition of $LaCrO_4$ and $Nd_{1-x}Ca_xCrO_4$ ($x=0$–0.2)

Ideal	Experimental
$LaCrO_4$	$La_{0.997(1)}Cr_{1.00}O_{3.99(1)}$
$NdCrO_4$ ($x=0$)	$Nd_{0.994(1)}Cr_{1.00}O_{3.99(2)}$
$Nd_{0.9}Ca_{0.1}CrO_4$ ($x=0.1$)	$Nd_{0.893(1)}Ca_{0.094(2)}Cr_{1.00}O_{3.98(1)}$
$Nd_{0.8}Ca_{0.2}CrO_4$ ($x=0.2$)	$Nd_{0.792(2)}Ca_{0.208(2)}Cr_{1.00}O_{3.99(1)}$

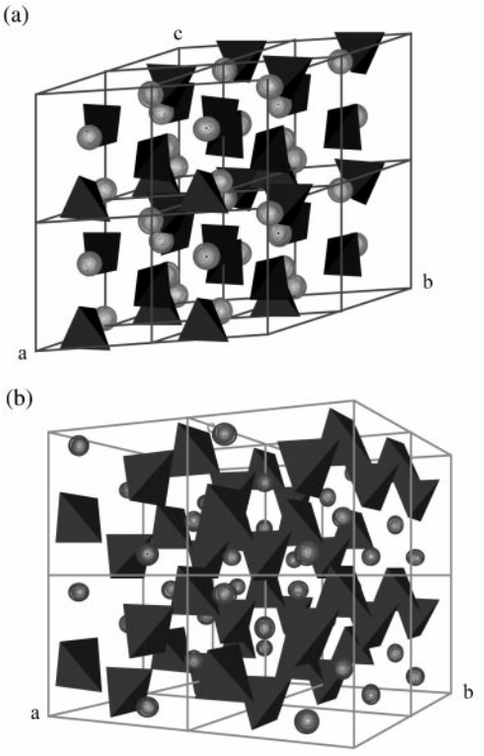

Fig. 1 Perspective projection of (a) monazite-type $LaCrO_4$ and (b) zircon-type $NdCrO_4$ in a $2\times2\times2$ unit cell. Gray spheres show lanthanide ions and tetrahedra are CrO_4^{3-} units.

The plots of the Seebeck coefficient, S, against the reciprocal of the temperature are shown in Fig. 3. The Seebeck coefficients for all compounds are larger than those observed for metallic materials and are within the range of commonly known semiconductors, a few tens to hundreds of μV K^{-1}.[21] In the measured temperature range, $LaCrO_4$ and $NdCrO_4$ have negative Seebeck coefficients, indicating that the main carriers are electrons. The values of S for these two oxides become less negative with increasing temperature. The temperature dependence of $Nd_{1-x}Ca_xCrO_4$ ($x=0.1$, 0.2) is small and opposite of $LaCrO_4$ and $NdCrO_4$, though the values are negative in the 300–600 K range.

At relatively high temperatures, the temperature dependence of the carrier mobility is known to be much smaller than that of the number of carriers, and carrier mobility can be disregarded in semiconductors.[21] The large temperature dependence of S for $LaCrO_4$ and $NdCrO_4$ suggests that the number of mobile electrons increases with increasing temperature. When mobility is approximated as constant in a finite temperature range, the Seebeck coefficient of an n-type semiconductor, S_n, is expressed by

$$S_n = -\left(\frac{E_c - E_F}{e}\frac{1}{T} + r\right) \quad (1)$$

where e is the electric charge on a electron, E_c is the potential at the bottom of the conduction band and E_F is the Fermi energy in an n-type semiconductor,[22] and r is a kinetic term which is assumed to be independent of temperature.[22] The Seebeck coefficients of $LaCrO_4$ and $NdCrO_4$ are proportional to the reciprocal of the temperature (Fig. 3) in agreement with eqn. (1). This indicates that electrons transport through a band in both compounds. West *et al.* have suggested that d^1 electrons in Li_3CrO_4 move by hopping directly between Cr sites, but no Seebeck voltage or other related properties were reported.[17] When an unpaired electron on Cr^{V} migrates to

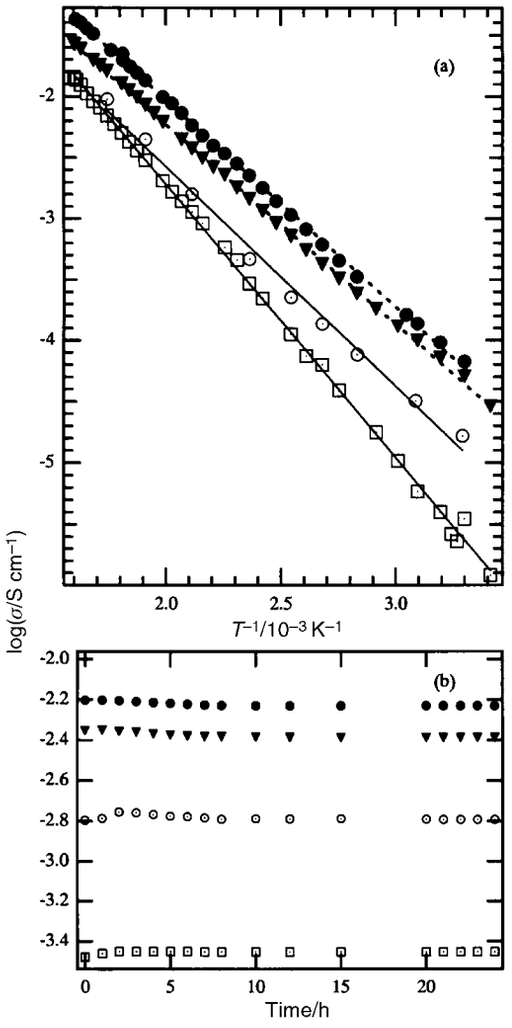

Fig. 2 (a) Arrhenius plots of the electric conductivity at 300–600 K, and (b) time dependence of electric conductivity at 473 K for $LaCrO_4$ (○), $NdCrO_4$ (□), $Nd_{0.9}Ca_{0.1}CrO_4$ (▼) and $Nd_{0.8}Ca_{0.2}CrO_4$ (●) in dry O_2.

neighboring localized Cr 3d orbitals by hopping in the two oxides here, the Seebeck coefficient, S_{hop}, is expressed by

$$S_{hop} = \frac{k}{e}\ln\left(\frac{n_e}{N_{loc} - n_e}\right) \quad (2)$$

where n_e and N_{loc} are the concentration of electrons and sites contributing to hopping transport with k the Boltzmann constant, all terms being independent of temperature at relatively high temperatures.[23] Therefore, if the hopping mechanism is controlling the conductivity, S_{hop} should be a small constant value in a specific temperature range.[23] This is inconsistent with the observed Seebeck coefficients for $LaCrO_4$ and $NdCrO_4$ in Fig. 3. The results up to 600 K suggest that the electric conductivity of $LaCrO_4$ and $NdCrO_4$ is due to a band-like transport of electrons, and not hopping between localized states. Accordingly, $LaCrO_4$ and $NdCrO_4$ may be categorized as intrinsic n-type semiconductors. It must be noted here that

Table 2 Electric conductivity at 300 K, σ_{300}, and activation energy, E_a, for $LaCrO_4$ and $Nd_{1-x}Ca_xCrO_4$ (x=0–0.2)

	σ_{300}/S cm^{-1}	E_a/kJ mol^{-1}
$LaCrO_4$	1.7×10^{-5}	18
$NdCrO_4$ (x=0)	2.4×10^{-6}	20
$Nd_{0.9}Ca_{0.1}CrO_4$ (x=0.1)	3.4×10^{-5}	15
$Nd_{0.8}Ca_{0.2}CrO_4$ (x=0.2)	6.9×10^{-5}	15

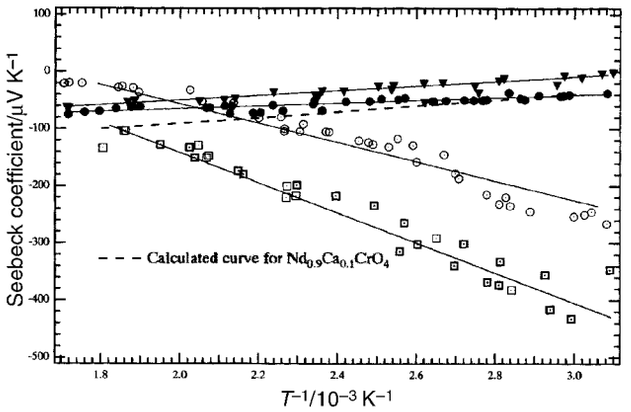

Fig. 3 Seebeck coefficients of $LaCrO_4$ (○), $NdCrO_4$ (□), $Nd_{0.9}Ca_{0.1}CrO_4$ (▼) and $Nd_{0.8}Ca_{0.2}CrO_4$ (●) as a function of the reciprocal temperature (300–600 K).

normally monazite-type and zircon-type oxides such as $LnXO_4$ ($Ln = La^{III}$–Lu^{III}, *etc.*, $X = V^V$, P^V, As^V, *etc.*) are insulators below 900 K.[24–26]

The conductivities of $LaCrO_4$ and $NdCrO_4$ can be expressed by

$$\sigma = e\mu_e N_e \exp\left(-\frac{E_g}{kT}\right) \quad (3)$$

where μ_e is the mobility of electrons, N_e is the total number of donor electrons, and E_g is the conductivity gap which is observed as the activation energy for $LaCrO_4$ and $NdCrO_4$ in Fig. 2(a).[22]

In $Nd_{1-x}Ca_xCrO_4$ (x=0.1 and 0.2), it is possible that the Cr^V–Cr^{VI} mixed valence states supply the charge exchange between the two valence states as hole hopping. The conductivity based on the hopping transport is given by

$$\sigma = A[n_e][N - n_e]T^{-3/2}\exp\left(-\frac{E_a}{kT}\right) \quad (4)$$

where A is a constant related to the probability of hopping and E_a is the activation energy of the hopping.[23] Arrhenius plots of σ for $Nd_{1-x}Ca_xCrO_4$ (x=0.1, 0.2) are shown in Fig. 2(a). These show good linear relationships between $\log\sigma$ and T^{-1} because of the small difference between $\log\sigma T$ and $\log\sigma$ in the narrow range of T^{-1} and are consistent with eqn. (4). The activation energy is about 15 kJ mol^{-1} for both. The Seebeck coefficients of $Nd_{1-x}Ca_xCrO_4$ (x=0.1 and 0.2) in Fig. 3, however, do not agree with eqn. (2). The Seebeck coefficients are negative at 300–600 K and become more negative with increasing temperature (Fig. 3), though the dependence is less significant. Consequently, it may be postulated that $Nd_{1-x}Ca_xCrO_4$ (x=0.1 and 0.2) are mixed conductors with both hole hopping and band-like transport of electrons. The net Seebeck coefficient, S_{tot}, for such a mixed conduction system is given by

$$S_{tot} = \frac{\sigma^+ S^+ + \sigma^- S^-}{\sigma^+ + \sigma^-} \quad (5)$$

where the superscripts + and – indicate terms arising from holes and electrons, respectively.[22] In $Nd_{1-x}Ca_xCrO_4$ (x=0.1, 0.2), the conduction of hole is by hopping, so that $S^- \gg S^+$. Then, eqn. (5) may be rewritten as eqn. (6).[21]

$$S_{tot} \approx \frac{\sigma^- S^-}{\sigma^+ + \sigma^-} \quad (6)$$

The terms σ^-, σ^+ and S^- are expressed by eqn. (7), (8) and (9) as

$$\sigma^- = \sigma_{e0}\exp\left(-\frac{E_g}{kT}\right) \qquad (\sigma_{e0} \equiv en\mu_e) \quad (7)$$

$$\sigma^{+} = \sigma_{h0} T^{-1} \exp\left(-\frac{E_a}{kT}\right) \quad (\sigma_{h0} \equiv A[n_e][N-n_e]) \tag{8}$$

$$S^{-} = -\left(S_{e0}\frac{1}{T} + S_{e1}\right) \quad \left(S_{e0} \equiv \frac{(E_c - E_F)}{e}, S_{e1} \equiv r\right) \tag{9}$$

$$\begin{aligned} S_{tot} &= \frac{-\sigma_{e0}\left(S_{e0}\frac{1}{T} + S_{e1}\right)\exp\left(-\frac{E_g}{kT}\right)}{\sigma_{e0}\exp\left(-\frac{E_g}{kT}\right) + \sigma_{h0}T^{-1}\exp\left(-\frac{E_a}{kT}\right)} \\ &\approx -\frac{\sigma_{e0}}{\sigma_{h0}}(S_{e0} + S_{e1}T)\exp\left(\frac{E_a - E_g}{kT}\right) \end{aligned} \tag{10}$$

Substituting eqn. (7)–(9) into eqn. (6), S_{tot} is expressed by eqn. (10).

The σ_{e0}, S_{e0} and S_{e1} terms correspond to the values for undoped $NdCrO_4$: σ_{e0} is estimated from the y-intercept of the Arrhenius plots of the conductivity; S_{e0} from the slope of the approximated line of the Seebeck coefficient; and S_{e1} from the y-intercept of this line. The σ_{h0} term can be estimated from the y-intercept of the Arrhenius plots of σT for $Nd_{1-x}Ca_xCrO_4$. Using these values of σ_{e0}, S_{e0}, S_{e1} and E_g for $NdCrO_4$, andσ_{h0} and E_a for $Nd_{1-x}Ca_xCrO_4$, the S_{tot} value can be calculated as a function of temperature. The result for $Nd_{1-x}Ca_xCrO_4$ ($x=0.1$) is shown as the broken line in Fig. 3. It does not coincide with the observed values but represents the change of Seebeck coefficient against temperature well.

The mixed valence $Nd_{1-x}Ca_xCrO_4$ ($x=0.1$ and 0.2) compounds are considered to be unique mixed conductors. The above results for $LaCrO_4$ and $Nd_{1-x}Ca_xCrO_4$ ($x=0$–0.2) indicate that Cr 3d states are degenerate and a relatively wide empty band extends above the degenerate states. The detailed conduction mechanism will be discussed below.

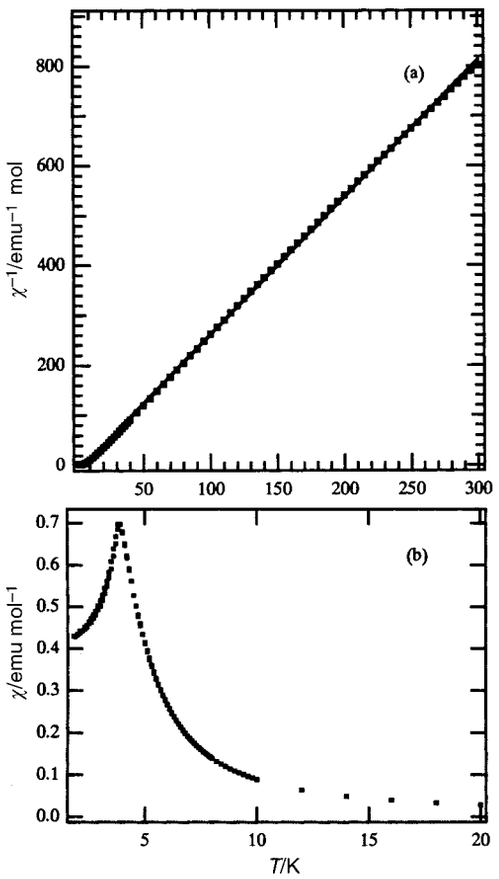

Fig. 4 (a) Temperature dependence of reciprocal molar susceptibility, χ^{-1}, and (b) molar susceptibility, χ, of $LaCrO_4$.

Table 3 Magnetic parameters of $LaCrO_4$ and $Nd_{1-x}Ca_xCrO_4$ ($x=0$–0.2)

	$\mu_{tot}{}^{o}/\mu_B$	$\mu_{Cr}{}^{o}/\mu_B$	θ/K
$LaCrO_4$	1.73	1.73	5.35
$NdCrO_4$ ($x=0$)	4.06	1.71	−48.6
$Nd_{0.9}Ca_{0.1}CrO_4$ ($x=0.1$)	3.91	1.63	−36.6
$Nd_{0.8}Ca_{0.2}CrO_4$ ($x=0.2$)	3.71	1.55	−42.1

Magnetic properies

The temperature dependence of the reciprocal molar susceptibility, χ^{-1}, for $LaCrO_4$ is shown in Fig. 4(a). In a very wide range from 20 to 300 K, $LaCrO_4$ obeys the Curie–Weiss law, consistent with the localized spin characteristics. The observed magnetic moment was $\mu_{Cr}{}^{o}=1.73$ μ_B (μ_B is a Bohr magneton) and the Curie temperature $\theta=5.35$ K. The observed magnetic moment is in good agreement with the theoretical magnetic moment for Cr^{V} ions, $\mu_{Cr}{}^{t}=1.72$ μ_B, indicating that the unpaired electrons remain localized on the Cr sublattices up to 300 K and probably also at higher temperatures. Below 20 K, the net molar susceptibility showed a maximum at 4.9 K, as shown in Fig. 4(b), indicating a typical antiferromagnetic transition.[27] These results indicate that antiferromagnetic ordering takes place due to interaction among Cr^{V} sublattices below the Néel temperature, 25 K. The magnetic parameters are summarized in Table 3.

The χ^{-1} *vs.* T plots obtained here for $Nd_{1-x}Ca_xCrO_4$ ($x=0$–

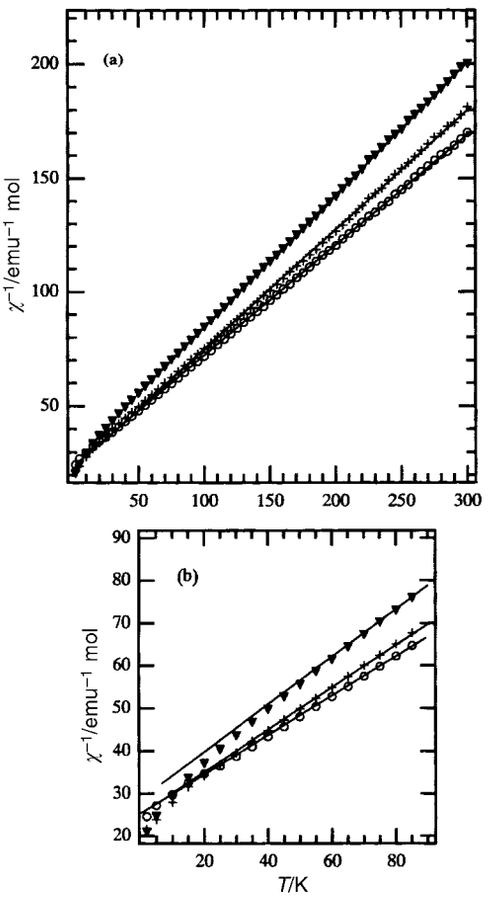

Fig. 5 Temperature dependence of reciprocal molar susceptibility, χ^{-1}, of $NdCrO_4$ (○), $Nd_{0.9}Ca_{0.1}CrO_4$ (+) and $Nd_{0.8}Ca_{0.2}CrO_4$ (▼) in the ranges (a) 2–300 K and (b) 2–90 K.

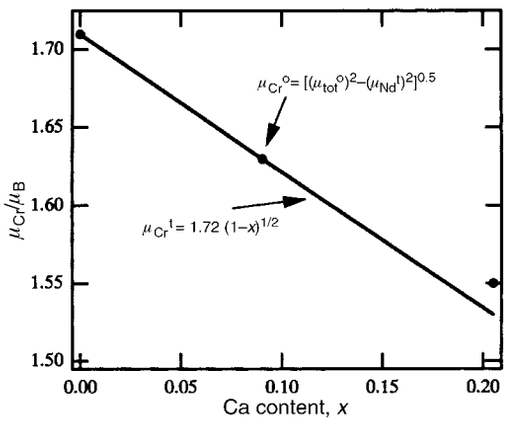

Fig. 6 Plots of the magnetic moment on Cr atoms in $Nd_{1-x}Ca_xCrO_4$ ($x=0$–0.2) as a function of calcium content, x. (●) and (—) show the observed moment, $\mu_{Cr}{}^o$ and the theoretical one, $\mu_{Cr}{}^t$, respectively.

0.2) are shown in Figs. 5(a) and (b), where the results of $NdCrO_4$ are consistent with the previous reports.[13,14] Above 50 K, $NdCrO_4$ also obeys the Curie–Weiss law, with a Curie temperature of $\theta=-48.6$ K. The negative Curie temperature and the downward deviation from the Curie–Weiss law below 50 K are due to antiferromagnetic interaction in the Cr^V sublattices. No apparent maximum due to the antiferromagnetic transition is observed in $NdCrO_4$ because there is no ordering in the Nd^{III} sublattices.[28] After correcting for the contribution of Nd^{III} ions with the $\mu_{Nd}{}^t$ (3.68 μ_B, reported by Van Vleck[29]) obtained from the observed total magnetic moment, $\mu_{tot}{}^o$, the $\mu_{Cr}{}^o$ of 1.71 μ_B agrees well with the $\mu_{Cr}{}^t$ in $LaCrO_4$. The magnetic behavior of $Nd_{1-x}Ca_xCrO_4$ ($x=0.1$, 0.2) resembles $NdCrO_4$; both obey the Curie–Weiss law above the Nèel temperature, and show an antiferromagnetic transition below the Nèel temperature. The $\mu_{Cr}{}^o$ value is calculated by eqn. (11) and plotted as a function of Ca content (analytical values in Table 1), x, in Fig. 6.

$$(\mu_{Cr}{}^o)^2=(\mu_{tot}{}^o)^2-(\mu_{Nd}{}^t)^2$$
$$(\mu_{Cr}{}^o)=\sqrt{(\mu_{tot}{}^o)^2-(1-x)\,(3.68)^2} \quad (11)$$

The $\mu_{Cr}{}^o$ decreases with increasing x, and lies on the $1.72(1-x)^{1/2}$ line in Fig. 6. These results indicate that the unpaired electrons are localized on the Cr atoms in all four compounds, and that Cr 3d states are degenerate.

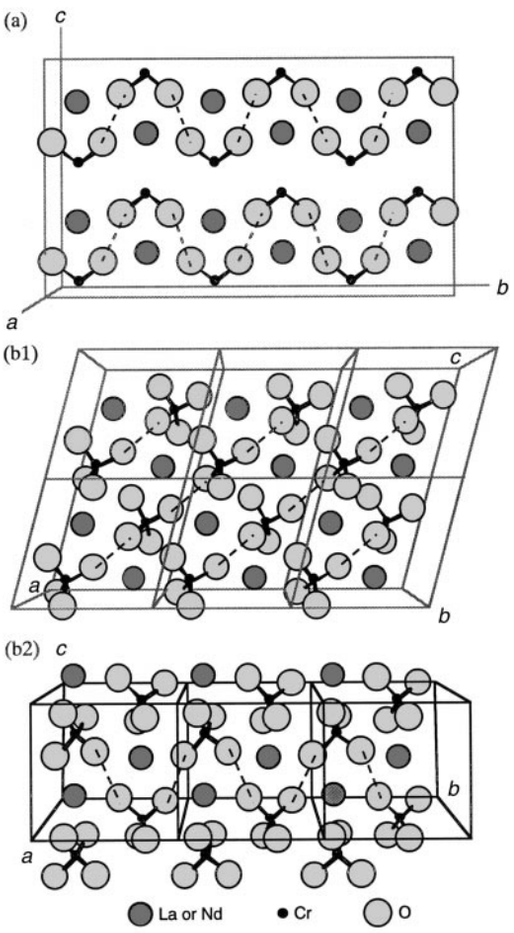

Fig. 7 Periodic short O–O arrays on (a) the 200 or 040 planes in $NdCrO_4$, and along (b1) the diagonals between the $-a$- and c-directions, and (b2) b-axis in $LaCrO_4$. The broken lines indicate the short O–O distances. Here, the size of all atoms was relatively reduced down to 50%.

The mechanism of electronic conduction

As described above, $LaCrO_4$ and $NdCrO_4$ behave as n-type semiconductors, while most monazite- and zircon-type oxides are insulators.[24–26] The electronic conduction of $LaCrO_4$ and $NdCrO_4$ can be explained by electrons being excited from degenerate states into the conduction band, through which electrons transport. Since both compounds have an unpaired electron of Cr^V in a d^1 configuration and the degeneration of the d states is indicated by the magnetic behavior, this unpaired electron must migrate. This model requires a wide empty band above the Fermi level. The contribution of the Ln 4f states to such a band can be neglected like with perovskite-type $LnMO_3$,[30] because the 4f states degenerate strongly and cannot form a wide band. The La sites in $LaCrO_4$ are strongly ionic, as reported for other monazite-type compounds like $LaPO_4$, $LaVO_4$ and others,[26,31,32] and the Cr 3d orbitals also cannot be expected to form a wide band in $LnCrO_4$. One reason why monazite- and zircon-type oxides are intrinsically insulators is that there is no linkage like the –O–Metal–O– link in the structure that could form a wide d band (Fig. 1). In $LaCrO_4$ and $Nd_{1-x}Ca_xCrO_4$ ($x=0$–0.2), the Cr 3d states are degenerate, as indicated by the results that holes in these states

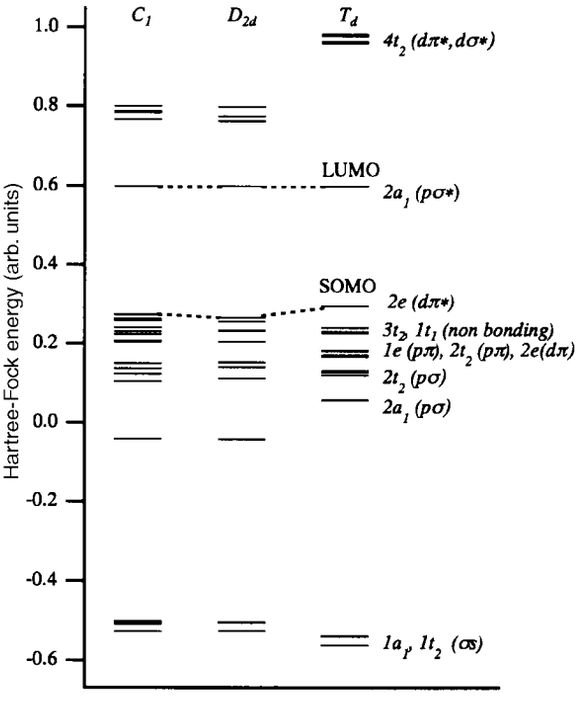

Fig. 8 Energy diagram of a MO for T_d, D_{2d} and C_1 symmetric $CrO_4{}^{3-}$ clusters, calculated by the HF/6-311G* method.

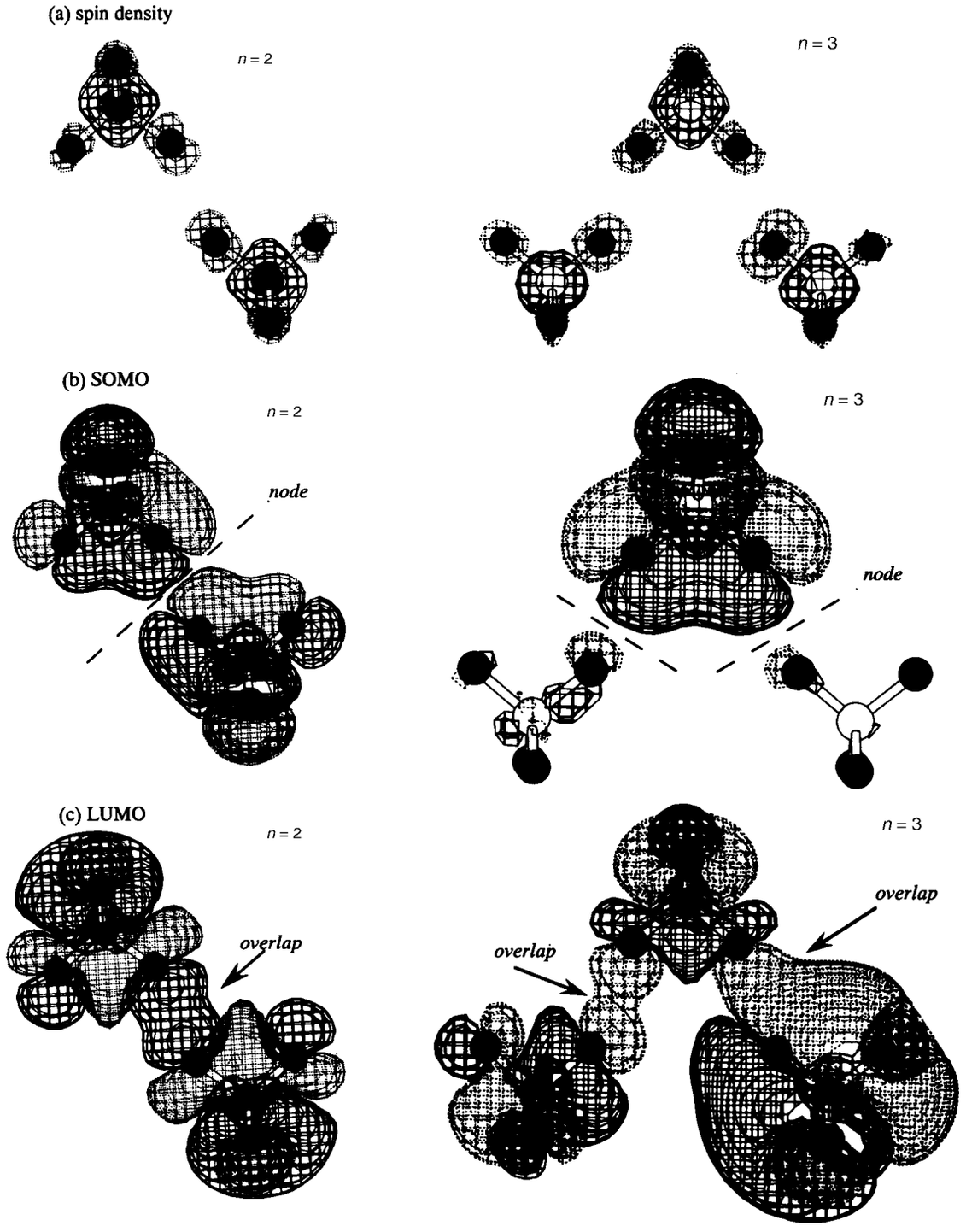

Fig. 9 Calculated spin densities on each atom (a), shape of the SOMO (b), and the LUMO (c) for the $(CrO_4^{3-})_n$ ($n=2$, 3) along the 200 or 040 planes in $NdCrO_4$. In (b) and (c), the solid and broken lines indicate the signs of wave function as + and −, respectively.

transport by the hopping mechanism in $Nd_{1-x}Ca_xCrO_4$ ($x=0.1$, 0.2) and as all compounds display Curie–Weiss magnetism, as shown in Figs. 2–5. Accordingly, a detailed explanation of why a conduction band forms must be attempted to explain the semiconductivity in $LnCrO_4$.

It is possible that a conduction band is formed by the contribution of the O 2p states. Generally, O 2p states do not form an empty conduction band, as the O 2p states are filled up in the ionic O^{2-} configuration. Considering the chemical and structural features of $LnCrO_4$, however, it is possible that an unpaired electron transports from one CrO_4^{3-} unit to a neighboring one through the O 2p orbital. Atanasov used the CI and CASSCF methods with the T_d symmetric $CrO_4^{3-}\cdot 4H^+$ cluster to calculate that the ratio of the ionic d^1 configuration was only 45% in the ground state, and that the ligand-to-metal charge-transfer (LMCT) states, mainly d^2L and d^3L^2 (L is a ligand hole) configurations, were intermixed in the ionic d^1 configuration.[33,34] This presents the possibility that the unoccupied O 2p states are created by LMCT states being intermixed in the ground state of $LnCrO_4$. As shown in Fig. 7, periodic short O–O′ arrays (the prime indicates the oxygen atom of the neighboring CrO_4^{3-} unit) are found in both the 200 and 040 planes [Fig. 7(a)] of $NdCrO_4$, and along the diagonals connecting between the *a*- and *c*-directions [Fig. 7(b1)], and the *b*-axis [Fig. 7(b2)] of $LaCrO_4$. The distances of these O–O′ arrays in Figs. 7(a), (b1) and (b2) are only 0.274, 0.271 and

0.292 nm, respectively,[9] and comparable to the 0.270 nm of a close-packed O–O distance (C.N. 2).[35] Therefore, it may be assumed that the conduction band of the antibonding O 2p states is created by intermixing of LMCT states and interaction between oxygen atoms of the neighboring CrO_4^{3-} units. The conduction band of $NaCuO_2$ containing the high valence state of Cu^{III} originates in the O 2p, where Cu^{III} causes the mixing of LMCT states such as d^9L or $d^{10}L^2$ into the ionic d^8 configuration in the ground state.[5] To justify this model, it is necessary to ensure that the HOMO (highest occupied molecular orbital) is of Cr 3d origin and that the LUMO (lowest unoccupied molecular orbital) is of O 2p origin in the ground state of a CrO_4^{3-} unit, and that HOMO localized on one unit and LUMO on the other overlap each other along short O–O arrays, as in Fig. 7.

The energy diagrams of molecular orbitals for CrO_4^{3-} clusters are shown in Fig. 8. The electronic configuration of a MO of a T_d symmeric cluster is described as shown in Fig. 8 by a population analysis using SCF density and referring to ref. 36 as follows:

$$(1a_1)^4\,(1t_2)^{12}\,(2a_1)^4\,(2t_2)^{12}\,(1e)^6\,(3t_2,1t_1)^{18}\,(2e)^2\,(2e)^1\,(2a_1)\,(4t_2)$$

Here, $1a_1$ and $1t_2$ (σs), $2a_1$, $2t_2$ and 1e ($p\sigma$ or $p\sigma^*$, $p\sigma + p\pi$ and $p\sigma$ respectively), $3t_2$ and t_1 (non-bonding p) all originate from oxygen; and 2e ($d\pi$ or $d\pi^*$) and $4t_2$ ($d\sigma^*$) mainly from chromium. It must be noted that the SOMO (singly occupied molecular orbital) is composed of Cr $d\pi^*$ states (2e), while the LUMO is identified as a $2a_1$ symmetric $p\sigma^*$ state of oxygen at the ground state. When the symmetry changes from T_d to D_{2d} and C_1, which are isomorphous with $NdCrO_4$ and $LaCrO_4$, respectively, the energy levels of the MOs were slightly changed but the electronic configurations did not change. These results indicate that some electrons on O 2p transfer onto Cr 3d, that the LMCT states are intermixed in the ground state. The energy diagrams in Fig. 8 are consistent with the report by Atanasov.[34]

The shapes of the spin density map, SOMO (π^* states) and LUMO (σ^* states), were calculated at the HF/STO-3G level for dimer and trimer models. The calculations were carried out without Nd^{3+} ions, using XRD data[9] for the atomic positions. The spin density on Cr atoms was +1.17 and on O atoms −0.04, indicating that unpaired electrons are mostly localized on the d orbital of Cr (SOMO) as shown in Fig. 9(a). Fig. 9(b) shows the equivalent isosurfaces of SOMOs in a dimer and in a trimer of the CrO_4^{3-} unit. In both clusters, the SOMO is created by the out-of-phase interaction between clusters: the orbitals of the CrO_4^{3-} unit in the clusters are completely separated by a node as shown in Fig. 9(b). The LUMO is widely delocalized above the clusters as shown in Fig. 9(c). These results strongly indicate that an unpaired electron in the

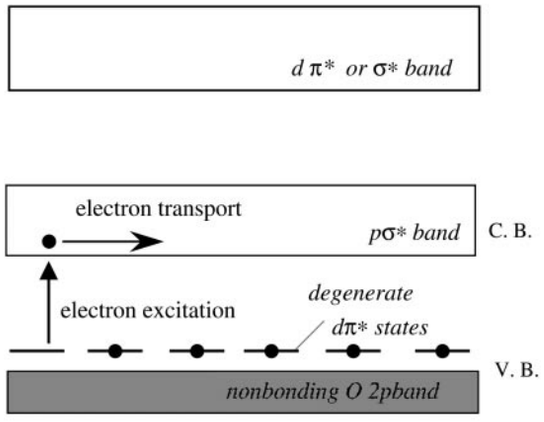

Fig. 10 Qualitative band model of $LaCrO_4$ and $Nd_{1-x}Ca_xCrO_4$ ($x=0$–0.2).

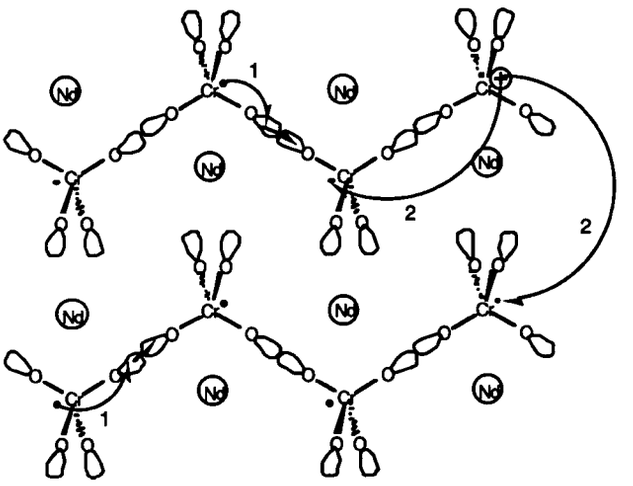

Fig. 11 Arrow 1, pathway for band-like electronic transport in $Nd_{1-x}Ca_xCrO_4$ ($x=0$–0.2), and arrow 2 for hole hopping in $Nd_{1-x}Ca_xCrO_4$ ($x=0.1$ and 0.2).

SOMO does not contribute to the electronic conductivity, whereas that in the LUMO is easily transferred to the conduction band composed of the LUMO and two low-lying excited states.

The structure of $LaCrO_4$ is very distorted and the calculations for a dimer and a trimer of CrO_4^{3-} units along the planes in Figs. 7(b1) and (b2) do not converge. The $p\sigma^*$ and $d\pi^*$ states in $LaCrO_4$, however, would be situated as in $NdCrO_4$, as seen in the experimental results in Figs. 2 and 3, and the chemical features do not show an apparent difference between the two.

Based on the experimental and calculated results, the band scheme for $LaCrO_4$ and $NdCrO_4$ is shown idealized in Fig. 10. The top of the valence band mainly consists of Cr $d\pi^*$ states, and the bottom of the conduction band of O $p\sigma^*$ states. The band in Fig. 10 leads to a mechanism of semiconductivity where the unpaired electrons on the Cr $d\pi^*$ states excite into the conduction band of the $p\sigma^*$ states and transport through that band. Fig. 9 and 10 show that in electronic conduction of $Nd_{1-x}Ca_xCrO_4$ ($x=0.1$, 0.2) hopping conduction of holes can occur between the degenerate $d\pi^*$ states together with band-like transport of electrons with a mechanism like that in $NdCrO_4$. The band model in Fig. 10 is not quantitative, but appears to be the most likely from the electronic and magnetic behaviors of all four compounds in the present work.

With the calculated shape of the SOMOs and LUMOs in Fig. 9 the conduction pathway in $NdCrO_4$ becomes much clearer and it spreads over the 200 and 040 planes. An unpaired electron on a Cr atom in the SOMO migrates onto an O atom, and it transfers to the O atom in the neighboring CrO_4^{3-} unit through the LUMO, as shown by arrow 1 in Fig. 11. This model accommodates the structural features of $NdCrO_4$ and $LaCrO_4$. The pathway with hole hopping in $Nd_{1-x}Ca_xCrO_4$ ($x=0.1$, 0.2) is described by arrow 2 in Fig. 11.

Conclusions

Monazite-type $LaCrO_4$ and zircon-type $NdCrO_4$ behave as semiconductors with activation energies of *ca.* 18 and 20 kJ mol^{-1}, respectively. Seebeck coefficients suggested that the main carriers in both compounds are electrons, which transport through the conduction band, and that both are n-type semiconductors. Mixed valence compounds, $Nd_{1-x}Ca_xCrO_4$ ($x=0.1$, 0.2), also behave as semiconductors, but two types of conduction—a band-like transport of electrons and a hopping of holes due to the mixed valences of the chromium—were found to occur together. The reciprocal of the magnetic

susceptibility of all the compounds obeyed Curie–Weiss law but the compounds had Nèel temperatures below which transition to antiferromagnetic ordering took place. This suggests that unpaired electrons from Cr^V ions remain localized on Cr atoms. The energy diagrams of the MO for CrO_4^{3-} clusters calculated by the HF/6-311G* method revealed that the LMCT states can intermix into the ionic d^1 configuration, because the LUMO can be assigned to the pσ* state (O 2p origin) and the HOMO to the dπ*. The structures of $LaCrO_4$ and $NdCrO_4$ would make the pσ* states advantageous in the creation of the conduction band because of the short distances between oxygen atoms in the neighboring CrO_4^{3-} units, which array periodically in particular planes or along specific directions in both compounds. The orbital shapes of the SOMO and LUMO and the spin densities were calculated for dimer and trimer models of the CrO_4^{3-} unit on the 200 plane of $NdCrO_4$. Most of the spin is localized on the Cr atoms in each model. The LUMO spreads throughout both the dimer and the trimer of the CrO_4^{3-} unit, while SOMOs have nodes and the orbitals of CrO_4^{3-} unit in the clusters are completely separated by these nodes. These results indicate that the pσ* states can form a wide conduction band and that the dπ* states are degenerate at the top of the valence band. Therefore, the mechanism of electronic conduction in $NdCrO_4$ is that the unpaired electrons on the degenerate dπ* states are excited into the pσ* band and transport through it, and the mechanism for $LaCrO_4$ will be the same. Electrons move from one CrO_4^{3-} unit to another through the overlapping pσ* states along the 200 plane. Mixed valence compounds, $Nd_{1-x}Ca_xCrO_4$ ($x=0.1$ and 0.2), show a mixed conduction mechanism where holes on chromium, introduced by the mixed valence, hop between the degenerate dπ* states acting together with the band-like transport of electrons. The LMCT states play an important role in creating the unoccupied O 2p states which enable electron conduction.

Acknowledgements

The authors thank Professor S. Maekawa, Dr S. Takahashi and Dr S. Ishihara of the Institute for Materials Research, Tohoku University, Japan, for constructive discussions on the mechanism of conduction. We also thank Professor Y. Hinatsu and Dr M. Wakeshima of the Graduate School of Science, Hokkaido University, Japan, who assisted in measuring the magnetic properties.

References

1 J. B. Torrence, P. Lacorre, A. I. Nazzal, P. W. Wang and T. C. Waung, *Phys. Rev. Sect. B*, 1992, **45**, 8209.
2 P. Lacorre, J. B. Torrence, J. Pannetier, A. I. Nazzal, P. W. Wang and T. C. Waung, *J. Solid State Chem.*, 1991, **91**, 225.
3 C. N. R. Rao, P. Ganguly, K. K. Shing and R. A. Mohan Ram, *J. Solid State Chem.*, 1998, **72**, 14.
4 J. B. Goodenough, N. F. Mott, M. Pouchard, G. Demezeau and P. Hagenmuller, *Mater. Res. Bull.*, 1973, **8**, 647.
5 T. Mizokawa, H. Namatame, A. Hujimori, K. Akeyama, H. Kondoh, H. Kuroda and N. Kosugi, *Phys. Rev. Lett.*, 1991, **67**, 1638.
6 Y. Takeda, R. Kanno, M. Noda and Y. Tomida, *J. Electrochem. Soc.*, 1987, **134**, 2656.
7 Y. Nakatani and M. Matsuoka, *Jpn. J. Appl. Phys.*, 1983, **22**, 233.
8 T. Tsuda, K. Nasu, A. Hujimori and K. Siratori, *Electric Conduction in Oxides*, Springer-Verlag, Heidelberg, 1991, pp. 40–220.
9 Y. Aoki, H. Konno, H. Tachikawa and M. Inagaki, *Bull. Chem. Soc. Jpn.*, 2000, **73**, 1197.
10 H. Konno, H. Tachikawa, A. Furusaki and R. Furuichi, *Anal. Sci.*, 1992, **8**, 641.
11 H. Schwarz, *Z. Anorg. Allg. Chem.*, 1963, **322**, 15.
12 H. Schwarz, *Z. Anorg. Allg. Chem.*, 1963, **322**, 129.
13 A. Morales-Sanchez, F. Fernandez and R. Saez-Puche, *J. Alloys Compd.*, 1993, **201**, 161.
14 H. Walter, H. G. Kahle, K. Mulder, H. C. Schopper and H. Schwarz, *Int. J. Magn.*, 1973, **5**, 129.
15 M. Steiner, H. Dachs and H. Ott, *Solid State Commun.*, 1979, **29**, 231.
16 G. Buisson, F. Tcheou, F. Sayetat and K. Scheuemann, *Solid State Commun.*, 1976, **18**, 871.
17 M. A. K. L. Dissanayake, S. Garcia-Martin, R. Saez-Puche, H. H. Sumathipala and A. R. West, *J. Mater. Chem.*, 1994, **4**, 1307.
18 Y. Aoki and H. Konno, *J. Solid State Chem.*, 2001, **156**, 370.
19 M. J. Frisch, G. W. Trucks, H. B. Schlegel, P. M. W. Gill, B. G. Johnson, M. A. Robb, J. R. Cheeseman, T. Keith, G. A. Petersson, J. A. Montgomery, K. Raghavachari, M. A. Al-Laham, V. G. Zakrzewski, J. V. Ortiz, J. B. Foresman, C. Y. Peng, P. Y. Ayala, W. Chen, M. W. Wong, J. L. Andres, E. S. Replogle, R. Gomperts, R. L. Martin, D. J. Fox, S. Binkley, D. J. Defrees, J. Baker, J. P. Stewart, M. Head-Gordon, C. Gonzalez and J. A. Pople, *GAUSSIAN98, Revision B.2*, Gaussian Inc., Pittsburgh, PA, 1998.
20 C. C. Roothan, *Rev. Mod. Phys.*, 1960, **32**, 179.
21 P. A. Cox, *The Electric Structure and Chemistry of Solid*, Oxford University Press, Oxford, 1987, pp. 20–129.
22 J. B. Goodenough, *Prog. Solid State Chem.*, 1971, **5**, 145.
23 H. Böttger and V. V. Bryksin, *Hopping Conduction in Solid*, VCH, Deerbeach, FL, 1985, pp. 51–87.
24 K. Gaur and H. B. Lal, *J. Mater. Sci.*, 1984, **19**, 3325.
25 K. Gaur and H. B. Lal, *J. Mater. Sci.*, 1985, **20**, 3167.
26 K. C. Mishra, I. Osterloh, H. Anton, B. Hannebauer, P. C. Schmidt and K. H. Johnson, *J. Mater. Res.*, 1997, **12**, 2183.
27 K. Adachi, *Magnetism of Compounds*., Shokabo, Tokyo, 1996, pp. 10–31.
28 K. Tetsuka, personal communication.
29 J. H. Van Vleck, *The Theory of Electric and Magnetic Susceptibilities*, Oxford University Press, Oxford, 1965, pp. 68–113.
30 K. Kamata, T. Nakamura and T. Sata, *J. Phys. Soc. Jpn.*, 1973, **120**, 73.
31 E. Nakazawa and F. J. Shiga, *Luminescence*, 1977, **15**, 255.
32 M. Greenblatt, J. H. Pifer, B. R. McGarvey and B. M. Wanklyn, *J. Chem. Phys.*, 1981, **74**, 6014.
33 M. Atanasov, H. Adamsky and K. Eifert, *J. Solid State Chem.*, 1997, **128**, 1.
34 M. Atanasov, *Z. Phys. Chem.*, 1997, **200**, 57.
35 R. D. Shannon and C. T. Prewitt, *Acta Crystallogr., Sect. B*, 1976, **32**, 751.
36 F. A. Cotton, *Chemical Applications of Group Theory*, John Wiley & Sons, USA, 1990, pp. 45–67.